A HIGH-ORDER PERTURBATION OF ENVELOPES (HOPE) METHOD FOR VECTOR ELECTROMAGNETIC SCATTERING BY PERIODIC INHOMOGENEOUS MEDIA: JOINT ANALYTICITY[*]

DAVID P. NICHOLLS[†] AND LIET VO[†]

Abstract. The scattering of electromagnetic waves by three-dimensional periodic structures is important for many problems of crucial scientific and engineering interest. Due to the complexity and three-dimensional nature of these waves, fast, accurate, and reliable numerical simulation of these are indispensable for engineers and scientists alike. For this, high-order spectral methods are frequently employed and here we describe an algorithm in this class. Our approach is perturbative in nature where we view the deviation of the permittivity from a constant value as the deformation and we pursue regular perturbation theory. More specifically, we expand the three-dimensional, vector-valued electric field in a Taylor series in this small deformation parameter, derive recursions that each term in this series must satisfy, invoke a novel elliptic theory to establish bounds on the size of each correction, and thereby show that the purported Taylor series does, in fact, converge. Beyond this, we show that each of these terms in the Taylor series is jointly analytic in all three spatial variables by estimating solutions of governing equations for derivatives of these terms. This work extends our previous contribution regarding the Helmholtz equation to the full vector Maxwell equations, by providing a rigorous analyticity theory, both in deformation size and spatial variable (provided that the permittivity is, itself, analytic).

1. Introduction. The scattering of electromagnetic waves by three-dimensional periodic structures is important for many problems of crucial scientific and engineering interest. Examples abound in areas as disparate as surface enhanced spectroscopy [26], extraordinary optical transmission [9], cancer therapy [10], and surface plasmon resonance (SPR) biosensing [17, 21, 24, 32].

Due to their central role in these nanotechnologies, simulations of these waves have been conducted with all of the classical numerical algorithms for approximating solutions to the relevant governing partial differential equations. This includes the finite difference [38, 23], finite element [20, 19], discontinuous Galerkin [16], spectral element [8], and spectral [15, 6, 4, 37] methods. While these are tempting choices, due to their *volumetric* nature they require a large number of unknowns ($N = N_x N_y N_z$ for a three-dimensional simulation) and mandate the inversion of large, nonsymmetric positive definite matrices (of dimension $N \times N$). Such properties are still an object of current study (for instance, see [11, 25]).

For the specific application of SPR sensors which we have in mind in the current contribution, their pervasiveness stems from two properties of an SPR, namely its extremely strong and sensitive response. More specifically, over the range of tens of

[†]Department of Mathematics, Statistics and Computer Science, University of Illinois at Chicago, Chicago, IL 60607 USA (davidn@uic.edu, lietvo@uic.edu).

nanometers in incident wavelength, the reflected energy can fall from nearly 100% by a factor of 10 or even 100 before returning to almost 100%. Obviously, to approximate such a structure with the required accuracy, the numerical algorithm should produce high fidelity results in a rapid and robust manner. For this reason we will focus upon high-order spectral (HOS) methods [15, 6, 4, 37] which can deliver precisely this behavior.

Returning to the classical approaches listed above, for the problem of scattering by homogeneous layers (which is one important avenue to generating SPRs) it is clearly unnecessary to discretize the bulk of each layer and state-of-the-art solvers seek interfacial unknowns with the knowledge that information inside the layers can readily be computed from appropriate integral formulas. Boundary element [36] and boundary integral [7, 22] methods are two such approaches and can produce spectrally accurate solutions in a fraction of the time of their volumetric competitors.

In previous work [27] the authors investigated a novel algorithm very much in the spirit of these HOS approaches, and inspired by the "high-order perturbation of surfaces" (HOPS) algorithms which have proven to be so appealing for layered media [30, 31]. A HOPS scheme is one which views the layer interfaces as perturbations of flat ones and then makes recursive corrections to the scattering returns from this classical, exactly solvable, configuration [39]. By contrast, our new "high-order perturbation of envelopes" (HOPE) schemes [27] consider a more general permittivity function, $\epsilon(x, y, z)$, which does not necessarily have layered structure. We followed the lead of Feng, Lin, and Lorton [13, 14] and adopted a perturbative philosophy (much like a HOPS algorithm) by viewing the permittivity as a perturbation of a trivial one, e.g.,

$$\epsilon(x, y, z) = \bar{\epsilon} - \delta(\bar{\epsilon}\mathcal{E}(x, y, z)), \quad \bar{\epsilon} \in \mathbf{R}^+, \quad \mathcal{E}(x + d_x, y + d_y, z) = \mathcal{E}(x, y, z),$$

where $\mathcal{E}$ is a permittivity "envelope." In this previous contribution we focused upon the two-dimensional scalar problems governing electromagnetic radiation in transverse electric (TE) and transverse magnetic (TM) polarizations. This new approach has computational advantages over volumetric solvers in certain configurations (e.g., where the support of $\mathcal{E}$ is small or where the set on which $\mathcal{E}$ significantly changes is small). A particular choice we pursued was an approximate indicator function which is nearly zero/unity to denote the absence/presence of a material.

Among the contributions of [27] was a new, extensive, and rigorous analysis. More specifically, we proved not only that the domain of analyticity of the scattered field in δ can be extended to a neighborhood of the *entire* real axis (up to topological obstruction), but also that this field is *jointly* analytic in parametric and spatial variables provided that $\mathcal{E}(x, y, z)$ is spatially analytic. In the current paper we extend some of these results to the three-dimensional vector electromagnetic case governed by the full time-harmonic Maxwell equations. More specifically, the scattered field is an outgoing, quasiperiodic solution of the time-harmonic Maxwell equations

$$\text{curl}\,[\text{curl}\,[E]] - \epsilon k_0^2 E = 0$$

(cf. (3.4)), which we show can be expanded in a *convergent* Taylor series

$$E = E(x, y, z; \delta) = \sum_{\ell=0}^{\infty} E_\ell(x, y, z)\delta^\ell$$

(cf. (4.2)), where the $E_\ell(x, y, z)$ are jointly analytic in (x, y, z) provided that $\mathcal{E}(x, y, z)$ is spatially analytic. The demonstration of these results required addressing both the vectorial *and* the three-dimensional nature of the scattered fields. This necessitated

the generalization of the relevant elliptic existence, uniqueness, and regularity result, and the derivation of more complicated source terms in the recursive problems due to the subtly coupled boundary conditions. We delay for future consideration the issue of the analytic continuation of our results to perturbations δ of arbitrary (real) size. (This requires an analysis of the variable coefficient Maxwell equations [3] which is more subtle than what we present here; however, we believe that this is a result which can be established with our current framework.) In the current contribution we also discuss a numerical method based upon the HOPE recursions that we used to establish these analyticity results, including the specification of an implementation that we used to simulate a scattering configuration with a known solution. Here also, we required highly nontrivial extensions of the results found in [27] as the vectorial and three-dimensional character of the solutions, coupled to the more involved boundary conditions, gave rise to a substantial increase in both the algorithmic and computational complexity of our implementation.

The rest of the paper is organized as follows. In section 2 we recall the governing equations complete with a discussion of transparent boundary conditions in section 3. We describe the HOPE algorithm in section 4 and begin our theoretical developments with a description of the relevant function spaces in section 5. We state and prove our results on parametric analyticity in section 6 and joint parametric/spatial analyticity in section 7. In section 8 we discuss our numerical results, featuring a discussion of our implementation in section 8.1 and the method of manufactured solutions (MMS) in section 8.2 (which delivers a configuration with known solution). In sections 8.3 and 8.4 we provide evidence of the stable and accurate behavior that our HOPE algorithm displays as the number of perturbation orders grows in the cases of small and large permittivity deviations, respectively. In section 8.5 we study the same question in the context of spatial refinement and, again, notice the robust and high-order nature of our method. In Appendix A we establish a joint analyticity result in the special case of lateral smoothness. (We provide the proofs of our new elliptic estimate and our novel numerical analysis in Sections SM1 and SM2 of the supplementary material (M164318_SM.pdf [local/web 310KB]).)

2. Governing equations. We consider materials modeled by the time-harmonic Maxwell equations in three dimensions with a constant permeability $\mu = \mu_0$ and no currents or sources,

$$(2.1) \qquad \operatorname{curl}[E] - i\omega\mu_0 H = 0, \quad \operatorname{curl}[H] + i\omega\epsilon E = 0,$$

where (E, H) are the electric and magnetic vector fields, and we have factored out time dependence of the form $\exp(-i\omega t)$ [3]. The permittivity $\epsilon(x, y, z)$ is biperiodic with periods d_x and d_y and is specified by

$$\epsilon(x, y, z) = \begin{cases} \epsilon^{(u)}\epsilon_0, & z > h, \\ \epsilon^{(v)}(x, y, z)\epsilon_0, & -h < z < h, \\ \epsilon^{(w)}\epsilon_0, & z < -h, \end{cases}$$

where ϵ_0 is the permittivity of vacuum, $\epsilon^{(u)}, \epsilon^{(w)} \in \mathbf{R}^+$, and $\epsilon^{(v)}(x + d_x, y + d_y, z) = \epsilon^{(v)}(x, y, z)$, and

$$\lim_{z \to h-} \epsilon^{(v)}(x, y, z) = \epsilon^{(u)}, \qquad \lim_{z \to (-h)+} \epsilon^{(v)}(x, y, z) = \epsilon^{(w)}.$$

For future use we can define

$$k_0^2 = \omega^2 \epsilon_0 \mu_0 = \frac{\omega^2}{c_0^2}, \quad (k^{(m)})^2 = \epsilon^{(m)} k_0^2, \quad m \in \{u, w\},$$

and $c_0 = 1/\sqrt{\epsilon_0 \mu_0}$ is the speed of light in vacuum.

This structure is illuminated from above by plane-wave incident radiation of the form

(2.2a) $$E^{\mathrm{inc}}(x,y,z) = A \exp(i\alpha x + i\beta y - i\gamma^{(u)}z),$$

(2.2b) $$H^{\mathrm{inc}}(x,y,z) = B \exp(i\alpha x + i\beta y - i\gamma^{(u)}z),$$

where

$$A \cdot \kappa = 0, \quad B = \frac{1}{\omega \mu_0} \kappa \times A, \quad |A| = |B| = 1,$$

and

$$\kappa = \begin{pmatrix} \alpha \\ \beta \\ -\gamma^{(u)} \end{pmatrix} = k^{(u)} \begin{pmatrix} \sin(\theta)\cos(\phi) \\ \sin(\theta)\sin(\phi) \\ -\cos(\theta) \end{pmatrix},$$

where (θ, ϕ) are the angles of incidence.

3. Transparent boundary conditions. Following our previous work [27] we aim to both rigorously specify the appropriate far-field boundary conditions and reduce the infinite domain to one of finite size. Conveniently, a variant of the scheme presented in Bao and Li [3] accomplishes both. In the upper domain $\{z > h\}$ we seek a solution as the sum of the incident radiation and an upward propagating (reflected) component, e.g.,

$$E = E^{\mathrm{inc}} + E^{\mathrm{refl}}$$
$$= A\exp(i\alpha x + i\beta y - i\gamma^{(u)}z) + c_{0,0}\exp(i\alpha x + i\beta y + i\gamma^{(u)}(z-h))$$
(3.1) $$\qquad + \sum_{(p,q)\neq(0,0)} \hat{u}_{p,q}\exp(i\alpha_p x + i\beta_q y + i\gamma_{p,q}^{(u)}(z-h))$$

[33, 39], where

$$\alpha_p = \alpha + (2\pi/d_x)p, \quad \beta_q = \beta + (2\pi/d_y)q,$$

$$\gamma_{p,q}^{(m)} := \begin{cases} \sqrt{\epsilon^{(m)}k_0^2 - \alpha_p^2 - \beta_q^2}, & \alpha_p^2 + \beta_q^2 \leq \epsilon^{(m)}k_0^2, \\ i\sqrt{\alpha_p^2 + \beta_q^2 - \epsilon^{(m)}k_0^2}, & \alpha_p^2 + \beta_q^2 > \epsilon^{(m)}k_0^2, \end{cases} \quad m \in \{u, w\},$$

since $\epsilon^{(u)}, \epsilon^{(w)} \in \mathbf{R}^+$. If we set $c_{0,0} = \hat{u}_{0,0} - A\exp(-i\gamma^{(u)}h)$, implying $\hat{u}_{0,0} = c_{0,0} + A\exp(-i\gamma^{(u)}h)$, then

$$E = A\exp(i\alpha x + i\beta y - i\gamma^{(u)}z) - A\exp(i\alpha x + i\beta y + i\gamma^{(u)}(z - 2h))$$
$$\qquad + \sum_{p=-\infty}^{\infty} \sum_{q=-\infty}^{\infty} \hat{u}_{p,q}\exp(i\alpha_p x + i\beta_q y + i\gamma_{p,q}^{(u)}(z-h)),$$

and $E(x,y,h) = u(x,y)$. It is a simple matter to show that

$$\partial_z E = (-i\gamma^{(u)})A\exp(i\alpha x + i\beta y - i\gamma^{(u)}z)$$
$$\qquad - (i\gamma^{(u)})A\exp(i\alpha x + i\beta y + i\gamma^{(u)}(z - 2h))$$
$$\qquad + \sum_{p=-\infty}^{\infty} \sum_{q=-\infty}^{\infty} \left(i\gamma_{p,q}^{(u)}\right)\hat{u}_{p,q}\exp\left(i\alpha_p x + i\beta_q y + i\gamma_{p,q}^{(u)}(z-h)\right),$$

so that

$$
\begin{aligned}
-\partial_z E(x,y,h) = {} & (i\gamma^{(u)})A\exp(i\alpha x + i\beta y - i\gamma^{(u)}h) \\
& + (i\gamma^{(u)})A\exp(i\alpha x + i\beta y + i\gamma^{(u)}(-h)) \\
& + \sum_{p=-\infty}^{\infty}\sum_{q=-\infty}^{\infty}\left(-i\gamma_{p,q}^{(u)}\right)\hat{u}_{p,q}\exp(i\alpha_p x + i\beta_q y).
\end{aligned}
$$

If we define the function

(3.2) $$ \phi(x,y) := \left(2i\gamma^{(u)}\exp(-i\gamma^{(u)}h)\right)A\exp(i\alpha x + i\beta y), $$

and the order-one Fourier multiplier (the externally directed Dirichlet–Neumann operator for the Maxwell equation on $\{z > h\}$)

$$
T_u[\psi] := \sum_{p=-\infty}^{\infty}\sum_{q=-\infty}^{\infty}\left(-i\gamma_{p,q}^{(u)}\right)\hat{\psi}_{p,q}\exp(i\alpha_p x + i\beta_q y),
$$

then we see that we can express the upward propagating condition [1] exactly with the boundary condition

$$
-\partial_z E(x,y,h) - T_u[E(x,y,h)] = \phi(x,y).
$$

In a similar fashion, in $\{z < -h\}$ we seek a solution which is purely downward propagating (transmitted)

(3.3) $$ E = E^{\text{trans}} = \sum_{p=-\infty}^{\infty}\sum_{q=-\infty}^{\infty}\hat{w}_{p,q}\exp\left(i\alpha_p x + i\beta_q y - i\gamma_{p,q}^{(w)}(z+h)\right) $$

[33, 39]. Clearly $E(x,y,-h) = w(x,y)$ and, with the calculation

$$
\partial_z E(x,y,-h) = \sum_{p=-\infty}^{\infty}\sum_{q=-\infty}^{\infty}\left(-i\gamma_{p,q}^{(w)}\right)\hat{w}_{p,q}\exp(i\alpha_p x + i\beta_q y),
$$

we define the analogous order-one Fourier multiplier (again, the externally directed Dirichlet–Neumann operator for the Helmholtz equation on $\{z < -h\}$)

$$
T_w[\psi] := \sum_{p=-\infty}^{\infty}\sum_{q=-\infty}^{\infty}\left(-i\gamma_{p,q}^{(w)}\right)\hat{\psi}_{p,q}\exp(i\alpha_p x + i\beta_q y),
$$

and we can state the downward propagating condition [1] transparently using

$$
\partial_z E(x,y,-h) - T_w[E(x,y,-h)] = 0.
$$

Eliminating the magnetic field from (2.1) and gathering our full set of governing equations we find the following problem to solve:

(3.4a) $\quad \text{curl}\,[\text{curl}\,[E]] - \epsilon^{(v)}k_0^2 E = 0 \qquad\qquad\qquad\qquad$ in S_v,

(3.4b) $\quad -\partial_z E - T_u[E] = \phi \qquad\qquad\qquad\qquad\qquad\quad$ at Γ_h,

(3.4c) $\quad \partial_z E - T_w[E] = 0 \qquad\qquad\qquad\qquad\qquad\qquad$ at Γ_{-h},

(3.4d) $\quad E(x+d_x, y+d_y, z) = \exp(i\alpha d_x + i\beta d_y)E(x,y,z),$

where

$$
S_v := (0,d_x)\times(0,d_y)\times(-h,h), \quad \Gamma_{\pm h} := (0,d_x)\times(0,d_y)\times\{z = \pm h\}.
$$

4. A high-order perturbation of envelopes method. Following the lead of our previous work [27] we do not pursue the solution of (3.4) by a classical volumetric approach, e.g. [3], but rather a perturbative one where we think of our configuration as a small deviation from a trivial structure,

$$(4.1) \qquad \epsilon^{(v)}(x,y,z) = \bar{\epsilon}\,(1 - \delta\mathcal{E}(x,y,z)) = \bar{\epsilon} - \delta(\bar{\epsilon}\mathcal{E}(x,y,z)),$$

where $\bar{\epsilon} \in \mathbf{R}^+$ is a constant, and $\delta \ll 1$. In our previous work on the Helmholtz equation in either TE or TM polarization, we showed that if $\mathcal{E}(x,z)$ is smooth enough, then the transverse components of E or H depend analytically upon δ. In light of this we posit that, for the full Maxwell equations which we consider here, the field $E = E(x,y,z;\delta)$ depends analytically upon δ so that

$$(4.2) \qquad E = E(x,y,z;\delta) = \sum_{\ell=0}^{\infty} E_\ell(x,y,z)\delta^\ell$$

converges strongly in a function space. It is not difficult to see that these E_ℓ must satisfy

$$(4.3a) \qquad \operatorname{curl}[\operatorname{curl}[E_\ell]] - \bar{\epsilon}k_0^2 E_\ell = -\bar{\epsilon}k_0^2 \mathcal{E} E_{\ell-1} \qquad \text{in } S_v,$$
$$(4.3b) \qquad -\partial_z E_\ell - T_u[E_\ell] = \delta_{\ell,0}\phi \qquad \text{at } \Gamma_h,$$
$$(4.3c) \qquad \partial_z E_\ell - T_w[E_\ell] = 0 \qquad \text{at } \Gamma_{-h},$$
$$(4.3d) \qquad E_\ell(x + d_x, y + d_y, z) = \exp(i\alpha d_x + i\beta d_y)E_\ell(x,y,z),$$

where $\delta_{\ell,0}$ is the Kronecker delta function. It is easy to see that

$$E_0(x,y,z) = Ae^{i\alpha x + i\beta y - i\bar{\gamma}z}, \quad \alpha^2 + \beta^2 + (\bar{\gamma})^2 = \bar{\epsilon}k_0^2,$$

and our HOPE scheme can be viewed as computing corrections to this by

$$E(x,y,z) = Ae^{i\alpha x + i\beta y - i\bar{\gamma}z} + \sum_{\ell=1}^{\infty} E_\ell(x,y,z)\delta^\ell.$$

There are many possibilities for the envelope function $\mathcal{E}(x,y,z)$ and each leads to a slightly different perturbation approach. For instance, consider the function

$$\Phi_{a,b}(z) := \frac{\tanh(w(z-a)) - \tanh(w(z-b))}{2},$$

with sharpness parameter w, which is effectively zero outside the interval (a,b) while being essentially one inside (a,b); cf. [27]. We can approximate a slab of material with thickness $2d$ and a gap of width $2g$ in vacuum by selecting

$$\bar{\epsilon} = 1, \quad \mathcal{E}(x,z) = \left(\frac{\bar{\epsilon} - \epsilon'}{\bar{\epsilon}}\right)\Phi_{-d,d}(z)\left\{1 - \Phi_{-g,g}(x)\right\}, \quad \delta = 1.$$

See Figure 4.1 with the choices $d = 1/4$, $g = 1/10$, and $w = 50$ on the cell $[-1,1] \times [-1,1]$.

5. Function spaces. In this section, we present function spaces and theoretical results that are necessary for our analysis later. We point out that due to the vectorial nature of the Maxwell equations, these are extensions of the results we utilized in our
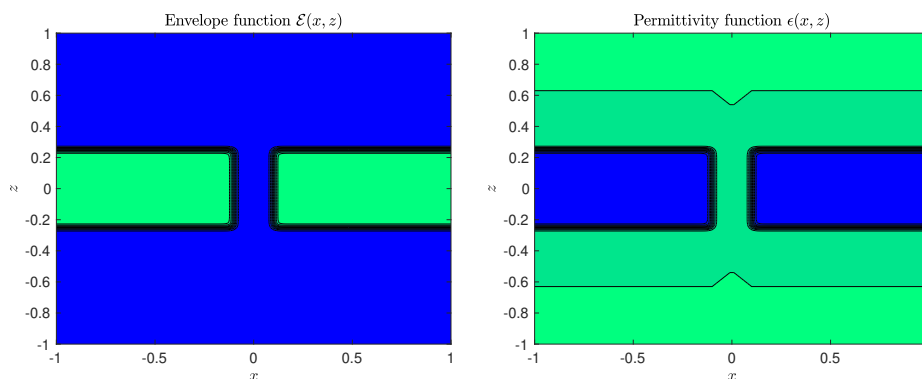
FIG. 4.1. *Contour plots of $\mathcal{E}(x,z)$ (left) and $\epsilon^{(v)}(x,z)$ (right).*

previous study [27]. For any real number $s \geq 0$, we have the classical interfacial quasiperiodic L^2 Sobolev norm

$$\|v\|_{H^s}^2 := \sum_{p=-\infty}^{\infty} \sum_{q=-\infty}^{\infty} \langle (p,q) \rangle^{2s} |\hat{v}_{p,q}|^2,$$
$$|\hat{v}_{p,q}|^2 = |\hat{v}_{p,q}^x|^2 + |\hat{v}_{p,q}^y|^2 + |\hat{v}_{p,q}^z|^2,$$

where

$$\langle (p,q) \rangle^2 := 1 + |p|^2 + |q|^2, \quad \hat{v}_{p,q}^j := \frac{1}{d_x d_y} \int_0^{d_x} \int_0^{d_y} v^j(x,y) e^{-i\alpha_p x - i\beta_q y} \, dx \, dy,$$

for $j \in \{x,y,z\}$. From this we define the interfacial quasiperiodic Sobolev space [22]

$$H^s(\Gamma) = \left\{ v(x,y) \in (L^2(\Gamma))^3 \mid \|v\|_{H^s} < \infty \right\}, \quad \Gamma := (0,d_x) \times (0,d_y).$$

In addition, we mention that the dual space of H^s, H^{-s}, can be defined by the norm above with a negative index. We also recall the space of s-times continuously differentiable scalar functions with Hölder norm

$$|g|_{C^s} := \max_{0 \leq \ell+r+t \leq s} \left| \partial_x^\ell \partial_y^r \partial_z^t g \right|_{L^\infty}.$$

Finally, we define the volumetric laterally quasiperiodic Sobolev space as

$$H^s(S_v) = \left\{ u(x,y,z) \in (L^2(S_v))^3 \mid \|u\|_{H^s} < \infty \right\},$$

where

$$\|u\|_{H^s}^2 := \sum_{j=0}^{s} \sum_{p=-\infty}^{\infty} \sum_{q=-\infty}^{\infty} \langle (p,q) \rangle^{2(s-j)} \int_{-h}^{h} |\partial_z^j \hat{u}_{p,q}(z)|^2 \, dz.$$

We close with an essential result [12, 28] required for our later proofs.

LEMMA 5.1. *Let $s \geq 0$ be an integer and D be either Γ or S_v. If $g \in C^s(D)$ and $w \in H^s(D)$, then $gw \in H^s(D)$ and*

$$\|gw\|_{H^s} \leq \tilde{M}(s,D) |g|_{C^s} \|w\|_{H^s},$$

where $\tilde{M}$ is some positive constant.

Furthermore, we recall the following elementary result [29, 27].

LEMMA 5.2. *Let $s \geq 0$ be an integer; then there exists a constant $S > 0$ such that*

$$\sum_{j=0}^{s} \frac{(s+1)^2}{(s-j+1)^2(j+1)^2} < S, \quad \sum_{j=0}^{s}\sum_{r=0}^{j} \frac{(s+1)^2}{(s-j+1)^2(j-r+1)^2(r+1)^2} < S^2.$$

6. Analyticity. At this point we are in a position to extend our previous results [27] by demonstrating the analytic dependence of the full electric field, $E = E(x, y, z; \delta)$, upon δ, sufficiently small. More specifically, we show that the expansion (4.2) converges strongly in an appropriate function space.

For this we require an elliptic estimate for our inductive proof which is established in Section SM1 of the supplementary material (M164318_SM.pdf [local/web 310KB]). For future convenience, we define the following differential operator associated to the Maxwell system:

$$\mathcal{L}_0 := \text{curl curl } - k_0^2 \bar{\epsilon}.$$

As is well known [3], the issue of *uniqueness* of solutions to the Maxwell problem

$$(6.1a) \qquad \mathcal{L}_0 V = 0 \qquad\qquad\qquad \text{in } S_v,$$
$$(6.1b) \qquad -\partial_z V - T_u[V] = 0 \qquad\qquad \text{at } \Gamma_h,$$
$$(6.1c) \qquad \partial_z V - T_w[V] = 0 \qquad\qquad \text{at } \Gamma_{-h},$$
$$(6.1d) \qquad V(x+d_x, y+d_y, z) = \exp(i\alpha d_x + i\beta d_y) V(x, y, z)$$

(cf. (4.3)), which should have only the *trivial* solution $V \equiv 0$, is a subtle one and certain illuminating frequencies ω will induce nonuniqueness in some configurations. Unfortunately a precise characterization of the set of forbidden frequencies is elusive and all that is known is that it is countable and accumulates at infinity [3]. To accommodate this state of affairs we define the set of permissible configurations

$$\mathcal{P} := \{(\omega, \bar{\epsilon}) \mid V \equiv 0 \text{ is the unique solution of } (6.1)\}.$$

With this we can now state the following fundamental elliptic regularity result.

THEOREM 6.1. *Given any integer $s \geq 0$, if $(\omega, \bar{\epsilon}) \in \mathcal{P}$, $F \in H^s(S_v)$, $\text{div}[F] \in H^{s+1}(S_v)$, $Q \in H^{s+1/2}(\Gamma)$, and $R \in H^{s+1/2}(\Gamma)$, then there exists a unique solution of*

$$(6.2a) \qquad \mathcal{L}_0 v = F \qquad\qquad\qquad \text{in } S_v,$$
$$(6.2b) \qquad -\partial_z v - T_u[v] = Q \qquad\qquad \text{at } \Gamma_h,$$
$$(6.2c) \qquad \partial_z v - T_w[v] = R \qquad\qquad \text{at } \Gamma_{-h},$$
$$(6.2d) \qquad v(x+d_x, y+d_y, z) = e^{i\alpha d_x + i\beta d_y} v(x, y, z),$$

satisfying

$$(6.3) \qquad \|v\|_{H^{s+2}} \leq C_e \left(\|F\|_{H^s} + \|\text{div}[F]\|_{H^{s+1}} + \|Q\|_{H^{s+1/2}} + \|R\|_{H^{s+1/2}} \right),$$

where $C_e > 0$ is a constant.

We can now prove our analyticity result.

THEOREM 6.2. *Given any integer $s \geq 0$, if $(\omega, \bar{\epsilon}) \in \mathcal{P}$, and $\mathcal{E} \in C^{s+2}(S_v)$ then the series (4.2) converges strongly. More precisely,*

$$(6.4) \qquad\qquad\qquad \|E_\ell\|_{H^{s+2}} \leq KB^\ell, \quad \forall\, \ell \geq 0,$$

for some constants $K, B > 0$.

Proof. We prove the estimate (6.4) by induction. For $\ell = 0$ the system (4.3) can be written as

$$
\begin{aligned}
&\mathcal{L}_0 E_0 = 0 && \text{in } S_v, \\
&-\partial_z E_0 - T_u[E_0] = \phi, && \text{at } \Gamma_h, \\
&\partial_z E_0 - T_w[E_0] = 0 && \text{at } \Gamma_{-h}, \\
&E_0(x + d_x, y + d_y, z) = e^{i\alpha d_x + i\beta d_y} E_0(x, y, z).
\end{aligned}
$$

So, we can apply Theorem 6.1 with $F \equiv 0$, $Q = \phi$, and $R \equiv 0$ to obtain

$$\|E_0\|_{H^{s+2}} \leq C_e \|\phi\|_{H^{s+1/2}} =: K.$$

Now, we assume that (6.4) is true for all $\ell < L$ and apply Theorem 6.1 to the system (4.3) for E_L with $F_L = -\bar{\epsilon} k_0^2 \mathcal{E} E_{L-1}$ and $Q_L \equiv R_L \equiv 0$. This gives

$$
\begin{aligned}
\|E_L\|_{H^{s+2}} &\leq C_e \left(\left\| \bar{\epsilon} k_0^2 \mathcal{E} E_{L-1} \right\|_{H^s} + \left\| \mathrm{div} \, \left[\bar{\epsilon} k_0^2 \mathcal{E} E_{L-1} \right] \right\|_{H^{s+1}} \right) \\
&\leq C_e k_0^2 |\bar{\epsilon}| 2 \left\| \mathcal{E} E_{L-1} \right\|_{H^{s+2}} \\
&\leq 2 C_e k_0^2 |\bar{\epsilon}| \tilde{M} \left| \mathcal{E} \right|_{C^{s+2}} \left\| E_{L-1} \right\|_{H^{s+2}} \\
&\leq 2 C_e k_0^2 |\bar{\epsilon}| \tilde{M} \left| \mathcal{E} \right|_{C^{s+2}} K B^{L-1} \\
&\leq K B^L,
\end{aligned}
$$

provided that

$$B > 2 C_e k_0^2 |\bar{\epsilon}| \tilde{M} \left| \mathcal{E} \right|_{C^{s+2}} . \qquad \square$$

From this we can derive the exponential order of convergence of the HOPE method. More precisely, defining the Lth partial sum of (4.2),

$$E^L(x, y, z) := \sum_{\ell=0}^{L} E_\ell(x, y, z) \delta^\ell,$$

we obtain the following error estimate for the HOPE method.

THEOREM 6.3. *If $(\omega, \bar{\epsilon}) \in \mathcal{P}$ and E is the unique solution of (3.4), under the assumptions of Theorem* 6.2 *we have the estimate*

$$\left\| E - E^L \right\|_{H^{s+2}} < \tilde{K}(B\delta)^{L+1},$$

for some constants $\tilde{K} > 0$ and $B > 2 C_e k_0^2 |\bar{\epsilon}| \tilde{M} \left| \mathcal{E} \right|_{C^{s+2}}$ provided that $|\delta| < 1/B$.

Proof. Since

$$E(x, y, z) - E^L(x, y, z) = \sum_{\ell=L+1}^{\infty} E_\ell(x, y, z) \delta^\ell,$$

we have, by Theorem 6.2,

$$\left\| E - E^L \right\|_{H^{s+2}} \leq \sum_{\ell=L+1}^{\infty} \|E_\ell\|_{H^{s+2}} \delta^\ell \leq \sum_{\ell=L+1}^{\infty} K B^\ell \delta^\ell.$$

By gathering terms and reindexing we have

$$\left\| E - E^L \right\|_{H^{s+2}} \leq K(B\delta)^{L+1} \sum_{\ell=0}^{\infty} (B\delta)^\ell \leq K \frac{(B\delta)^{L+1}}{1 - (B\delta)} \leq \tilde{K}(B\delta)^{L+1}$$

for $|B\delta| < 1$, where we have used the elementary fact that

$$\sum_{\ell=0}^{\infty} \alpha^\ell = \frac{1}{1 - \alpha}$$

provided that $|\alpha| < 1$. □

Remark 6.1. A careful inspection of our result seems to indicate that the applicability of our method is extremely limited in the high-frequency regime as we require

$$|\delta| < \frac{1}{B} = \frac{1}{2C_e k_0^2 |\bar{\epsilon}| \tilde{M} |\mathcal{E}|_{C^{s+2}}}.$$

Without taking into account the k_0 dependence of C_e, it would appear that the disk of analyticity is proportional to k_0^{-2} as $k_0 \to \infty$ which is quite restrictive. However, as we plan to show in a future publication, the domain of analyticity contains a neighborhood of the *entire* real axis so that, provided one can access this via suitable analytic continuation technique (e.g., Padé approximation [2]), deformations of *any* size can be accommodated.

7. Joint analyticity. We close our theoretical developments with a result on *joint* analyticity of the scattered field with respect to not only the perturbation parameter δ, but also the spatial coordinates (x, y, z). As with the analogous result for the Helmholtz equation found in [27], this will require analyticity of the permittivity envelope function $\mathcal{E}(x, y, z)$. More precisely, we will show that the E_ℓ from (4.2) satisfy conditions analogous to those in the following definition of analyticity.

DEFINITION 7.1. *Given an integer $m \geq 0$, if the functions $f = f(x, y)$ and $\mathcal{E} = \mathcal{E}(x, y, z)$ are real analytic and satisfy the estimates*

$$\left| \frac{\partial_x^r \partial_y^t}{(r+t)!} f \right|_{C^m} \leq C_f \frac{\eta^r}{(r+1)^2} \frac{\theta^t}{(t+1)^2},$$

$$\left| \frac{\partial_x^r \partial_y^t \partial_z^s}{(r+t+s)!} \mathcal{E} \right|_{C^m} \leq C_{\mathcal{E}} \frac{\eta^r}{(r+1)^2} \frac{\theta^t}{(t+1)^2} \frac{\zeta^s}{(s+1)^2},$$

for all $r, t, s \geq 0$, for some constants $C_f, C_{\mathcal{E}}, \eta, \theta, \zeta > 0$, then $f \in C_m^\omega(\Gamma)$ and $\mathcal{E} \in C_m^\omega(S_v)$.

The space C_m^ω is the space of real analytic functions with radius of convergence (specified by η, θ, and ζ) measured in the C^m norm. It is clear that the incident radiation function ϕ, (3.2), is jointly analytic in x and y as we now explicitly state.

LEMMA 7.2. *The function*

$$\phi(x, y) := (2i\gamma^{(u)} \exp(-i\gamma^{(u)} h)) A \exp(i\alpha x + i\beta y)$$

is real analytic and satisfies

$$\left\| \frac{\partial_x^r \partial_y^t}{(r+t)!} \phi \right\|_{H^{1/2}} \leq C_\phi \frac{\eta^r}{(r+1)^2} \frac{\theta^t}{(t+1)^2},$$

for all $r, t \geq 0$, for some constants $C_\phi, \eta, \theta > 0$.

Now we present the fundamental elliptic estimate (proven in Appendix A) which is required in our following proof.

THEOREM 7.3. *Given any integer $m \geq 0$, if $(\omega, \bar{\epsilon}) \in \mathcal{P}$, $F(x, y, z) \in C_m^\omega(S_v)$ such that*

$$\max\left\{\left\|\frac{\partial_x^r \partial_y^t \partial_z^s}{(r+t+s)!} F\right\|_{H^0}, \left\|\frac{\partial_x^r \partial_y^t \partial_z^s}{(r+t+s)!}\mathrm{div}\,[F]\right\|_{H^1}\right\} \leq C_F \frac{\eta^r}{(r+1)^2}\frac{\theta^t}{(t+1)^2}\frac{\zeta^s}{(s+1)^2}$$

for all $r, t, s \geq 0$ and for some constants $C_F, \eta, \theta, \zeta > 0$, and $Q, R \in C_m^\omega(\Gamma))$ satisfying

$$\left\|\frac{\partial_x^r \partial_y^t}{(r+t)!} Q\right\|_{H^{1/2}} \leq C_Q \frac{\eta^r}{(r+1)^2}\frac{\theta^t}{(t+1)^2},$$

$$\left\|\frac{\partial_x^r \partial_y^t}{(r+t)!} R\right\|_{H^{1/2}} \leq C_R \frac{\eta^r}{(r+1)^2}\frac{\theta^t}{(t+1)^2}$$

for all $r, t \geq 0$ and some constants $C_R, C_Q > 0$, then there exists a unique solution $v \in C_m^\omega(S_v)$ of

$$\begin{aligned}
\mathcal{L}_0 v &= F && in\ S_v,\\
-\partial_z v - T_u[v] &= Q && at\ \Gamma_h,\\
\partial_z v - T_w[v] &= R && at\ \Gamma_{-h},\\
v(x + d_x, y + d_y, z) &= e^{i\alpha d_x + i\beta d_y} v(x, y, z),
\end{aligned}$$

satisfying

$$(7.1) \qquad \left\|\frac{\partial_x^r \partial_y^t \partial_z^s}{(r+t+s)!} v\right\|_{H^2} \leq \underline{C}_e \frac{\eta^r}{(r+1)^2}\frac{\theta^t}{(t+1)^2}\frac{\zeta^s}{(s+1)^2},$$

for all $r, t, s \geq 0$, where

$$\underline{C}_e = \overline{C}(h)(C_F + C_Q + C_R) > 0,$$

and $\overline{C}(h) > 0$ is a constant.

We now give the recursive estimate which is essential for our joint analyticity result.

LEMMA 7.4. *For any integer $m > 0$, if $\mathcal{E} \in C_m^\omega(S_v)$ such that*

$$\left|\frac{\partial_x^r \partial_y^t \partial_z^s}{(r+t+s)!} \mathcal{E}\right|_{C^m} \leq C_\mathcal{E} \frac{\eta^r}{(r+1)^2}\frac{\theta^t}{(t+1)^2}\frac{\zeta^s}{(s+1)^2}$$

for all $r, t, s \geq 0$ and some constants $C_\mathcal{E}, \eta, \theta, \zeta > 0$, and

$$\left\|\frac{\partial_x^r \partial_y^t \partial_z^s}{(r+t+s)!} E_\ell\right\|_{H^2} \leq KB^\ell \frac{\eta^r}{(r+1)^2}\frac{\theta^t}{(t+1)^2}\frac{\zeta^s}{(s+1)^2}, \quad \forall\,\ell < L,$$

for all $r, t, s \geq 0$ and for some constants $K, B > 0$, then

$$\max\left\{\left\|\frac{\partial_x^r \partial_y^t \partial_z^s}{(r+t+s)!} F_L\right\|_{H^0}, \left\|\frac{\partial_x^r \partial_y^t \partial_z^s}{(r+t+s)!}\mathrm{div}\,[F_L]\right\|_{H^1}\right\}$$

$$\leq \tilde{C} K B^{L-1} \frac{\eta^r}{(r+1)^2}\frac{\theta^t}{(t+1)^2}\frac{\zeta^s}{(s+1)^2}$$

for all $r, t, s \geq 0$ and some constant $\tilde{C} > 0$.

Proof. Recall that

$$F_L = -\bar{\epsilon} k_0^2 \mathcal{E} E_{L-1},$$

so, using Leibniz's rule, we obtain

$$\frac{\partial_x^r \partial_y^t \partial_z^s}{(r+t+s)!} F_L$$
$$= -\frac{k_0^2 \bar{\epsilon} r! t! s!}{(r+t+s)!} \sum_{j=0}^{r} \sum_{k=0}^{t} \sum_{\ell=0}^{s} \left(\frac{\partial_x^{r-j}}{(r-j)!} \frac{\partial_y^{t-k}}{(t-k)!} \frac{\partial_z^{s-\ell}}{(s-\ell)!} \mathcal{E} \right) \left(\frac{\partial_x^j}{j!} \frac{\partial_y^k}{k!} \frac{\partial_z^\ell}{\ell!} E_{L-1} \right).$$

Using the inequality $r! t! s! \leq (r+t+s)!$ and

$$\max \left\{ \left\| \frac{\partial_x^r \partial_y^t \partial_z^s}{(r+t+s)!} F_L \right\|_{H^0}, \left\| \frac{\partial_x^r \partial_y^t \partial_z^s}{(r+t+s)!} \text{div } [F_L] \right\|_{H^1} \right\} \leq \left\| \frac{\partial_x^r \partial_y^t \partial_z^s}{(r+t+s)!} F_L \right\|_{H^2},$$

we obtain

$$\left\| \frac{\partial_x^r \partial_y^t \partial_z^s}{(r+t+s)!} F_L \right\|_{H^2}$$
$$\leq \bar{\epsilon} k_0^2 \sum_{j=0}^{r} \sum_{k=0}^{t} \sum_{\ell=0}^{s} \left\| \left(\frac{\partial_x^{r-j}}{(r-j)!} \frac{\partial_y^{t-k}}{(t-k)!} \frac{\partial_z^{s-\ell}}{(s-\ell)!} \mathcal{E} \right) \left(\frac{\partial_x^j}{j!} \frac{\partial_y^k}{k!} \frac{\partial_z^\ell}{\ell!} E_{L-1} \right) \right\|_{H^2}$$
$$\leq \bar{\epsilon} k_0^2 \sum_{j=0}^{r} \sum_{k=0}^{t} \sum_{\ell=0}^{s} \tilde{M} \left| \frac{\partial_x^{r-j}}{(r-j)!} \frac{\partial_y^{t-k}}{(t-k)!} \frac{\partial_z^{s-\ell}}{(s-\ell)!} \mathcal{E} \right|_{C^2}$$
$$\times \left\| \frac{\partial_x^j}{j!} \frac{\partial_y^k}{k!} \frac{\partial_z^\ell}{\ell!} E_{L-1} \right\|_{H^2}$$
$$\leq \bar{\epsilon} k_0^2 \tilde{M} \sum_{j=0}^{r} \sum_{k=0}^{t} \sum_{\ell=0}^{s} C_{\mathcal{E}} \frac{\eta^{r-j}}{(r-j+1)^2} \frac{\theta^{t-k}}{(t-k+1)^2} \frac{\zeta^{s-\ell}}{(s-\ell+1)^2}$$
$$\times KB^{L-1} \frac{\eta^j}{(j+1)^2} \frac{\theta^k}{(k+1)^2} \frac{\zeta^\ell}{(\ell+1)^2}$$
$$= \bar{\epsilon} k_0^2 C_{\mathcal{E}} \tilde{M} KB^{L-1} \frac{\eta^r}{(r+1)^2} \frac{\theta^t}{(t+1)^2} \frac{\zeta^s}{(s+1)^2}$$
$$\times \sum_{j=0}^{r} \frac{(r+1)^2}{(r-j+1)^2(j+1)^2} \sum_{k=0}^{t} \frac{(t+1)^2}{(t-k+1)^2(k+1)^2}$$
$$\times \sum_{\ell=0}^{s} \frac{(s+1)^2}{(s-\ell+1)^2(\ell+1)^2}$$
$$\leq \bar{\epsilon} k_0^2 C_{\mathcal{E}} \tilde{M} S^3 KB^{L-1} \frac{\eta^r}{(r+1)^2} \frac{\theta^t}{(t+1)^2} \frac{\zeta^s}{(s+1)^2},$$

where S is a positive constant such that

$$\sum_{j=0}^{r} \frac{(r+1)^2}{(r-j+1)^2(j+1)^2} < S \quad \forall \, r \geq 0;$$

cf. Lemma 5.2. Therefore, the proof is complete by choosing

$$\tilde{C} \geq \bar{\epsilon} k_0^2 C_{\mathcal{E}} \tilde{M} S^3. \qquad \Box$$

We conclude with our joint analyticity theorem.

THEOREM 7.5. *Given any integer $m > 0$, if $(\omega, \bar{\epsilon}) \in \mathcal{P}$, and $\mathcal{E} \in C_m^\omega(S_v)$ such that*

$$\left| \frac{\partial_x^r \partial_y^t \partial_z^s}{(r+t+s)!} \mathcal{E} \right|_{C^m} \leq C_{\mathcal{E}} \frac{\eta^r}{(r+1)^2} \frac{\theta^t}{(t+1)^2} \frac{\zeta^s}{(s+1)^2}$$

for all $r, t, s \geq 0$ and some constants $C_{\mathcal{E}}, \eta, \theta, \zeta > 0$, then the series (4.2) converges strongly. Moreover the $E_\ell(x, y, z)$ satisfy the joint analyticity estimate

$$(7.2) \qquad \left\| \frac{\partial_x^r \partial_y^t \partial_z^s}{(r+t+s)!} E_\ell \right\|_{H^2} \leq K B^\ell \frac{\eta^r}{(r+1)^2} \frac{\theta^t}{(t+1)^2} \frac{\zeta^s}{(s+1)^2}$$

for all $\ell, r, t, s \geq 0$ and some constants $K, B > 0$.

Proof. We prove (7.2) by induction, beginning with $\ell = 0$. Applying Theorem 7.3 with $F \equiv 0$, $Q = \phi$, and $R \equiv 0$ we obtain

$$\left\| \frac{\partial_x^r \partial_y^t \partial_z^s}{(r+t+s)!} E_0 \right\|_{H^2} \leq K \frac{\eta^r}{(r+1)^2} \frac{\theta^t}{(t+1)^2} \frac{\zeta^s}{(s+1)^2}$$

for all $r, t, s \geq 0$, where $K = \overline{C}(h) C_\phi$. Next we assume that (7.2) is valid for all $\ell < L$ which implies

$$\max \left\{ \left\| \frac{\partial_x^r \partial_y^t \partial_z^s}{(r+t+s)!} E_\ell \right\|_{H^0}, \left\| \frac{\partial_x^r \partial_y^t \partial_z^s}{(r+t+s)!} \mathrm{div}\ [E_\ell] \right\|_{H^1} \right\}$$
$$\leq K B^\ell \frac{\eta^r}{(r+1)^2} \frac{\theta^t}{(t+1)^2} \frac{\zeta^s}{(s+1)^2} \quad \forall\ \ell < L.$$

With $\ell = L$ we invoke Lemma 7.4 and apply Theorem 7.3 with $F \equiv F_L$, $C_F = \tilde{C} K B^{L-1}$, $Q \equiv 0$, and $R \equiv 0$, to arrive at

$$\left\| \frac{\partial_x^r \partial_y^t \partial_z^s}{(r+t+s)!} E_L \right\|_{H^2} \leq \overline{C}(h) \tilde{C} K B^{L-1} \frac{\eta^r}{(r+1)^2} \frac{\theta^t}{(t+1)^2} \frac{\zeta^s}{(s+1)^2} \quad \forall r, t, s \geq 0.$$

The proof is complete by choosing $B > \overline{C}(h) \tilde{C}$. $\qquad \square$

8. Numerical results. We now present numerical results of an implementation of the HOPE recursions, (4.3), which demonstrate the accurate and stable results one can obtain with this algorithm. We will see that for smooth envelopes (e.g., $\mathcal{E}$ analytic) our method yields accurate solutions in a robust and efficient manner.

8.1. Implementation. We have produced a concrete instance of the HOPE algorithm which begins with a truncation of the expansion (4.2) at order $\ell = L$,

$$(8.1) \qquad E(x, y, z; \delta) \approx E^L(x, y, z; \delta) := \sum_{\ell=0}^{L} E_\ell(x, y, z) \delta^\ell.$$

Each of the functions E_ℓ should approximately satisfy (4.3) which we accomplish with a HOS method [15, 6, 4, 37]. Due to the quasiperiodic lateral boundary conditions, we used a Fourier–Chebyshev method which makes the approximation

$$E_\ell \approx E_\ell^{N_x, N_y, N_z} := \sum_{p=-N_x/2}^{N_x/2-1} \sum_{q=-N_y/2}^{N_y/2-1} \sum_{r=0}^{N_z} \hat{E}_{\ell,p,q,r} T_r(z/h) e^{i\alpha_p x + i\beta_q y}, \quad \hat{E}_{\ell,p,q,r} \in \mathbf{C}^3,$$

and T_r is the rth Cheybshev polynomial. To find the unknowns $\hat{E}_{\ell,p,q,r}$ we adopt the collocation approach which demands that the equations (4.3) be true at the gridpoints

$$\{x_j = j(d_x/N_x) \mid 0 \le j \le N_x - 1\}, \quad \{y_k = k(d_y/N_y) \mid 0 \le k \le N_y - 1\},$$
$$\{z_m = h\cos(\pi m/N_z) \mid 0 \le m \le N_z\}.$$

This delivers a system of linear equations which can be resolved in an efficient and stable manner with the repeated use of fast Fourier and Chebyshev transforms [15, 6, 4, 37].

Remark 8.1. A rigorous numerical analysis of this method can be conducted very much in the spirit of [18]. In Section SM2 of the supplementary material (M164318_SM.pdf [local/web 310KB]) we begin this study and are able to establish the following result.

THEOREM 8.1. *Let E be the solution of the full Maxwell system,* (3.4), *and let* $r \ge 2$, *then*

$$\left\| E - E^{L,N_x,N_y,N_z} \right\|_{L^2} \lesssim (B\delta)^{L+1} + (N_x^{1-r} + N_y^{1-r} + N_z^{1-r}) \left\| \phi \right\|_{H^{r+1/2}},$$

for any constant

$$B > C_e k_0^2 \bar{\epsilon} \tilde{M} \left| \mathcal{E} \right|_{C^s},$$

giving convergence for $\delta < 1/B$.

8.2. The method of manufactured solutions. To test the validity of our implementation, we utilized the MMS [5, 34, 35]. To describe this, consider the general system of partial differential equations subject to generic boundary conditions

$$\mathcal{P}v = 0 \qquad\qquad \text{in } \Omega,$$
$$\mathcal{B}v = 0 \qquad\qquad \text{at } \partial\Omega.$$

It is typically just as easy to implement a numerical algorithm to solve the nonhomogeneous version of this set of equations

$$\mathcal{P}v = \mathcal{F} \qquad\qquad \text{in } \Omega,$$
$$\mathcal{B}v = \mathcal{J} \qquad\qquad \text{at } \partial\Omega.$$

To validate our code we began with the "manufactured solution," $\tilde{v}$, and set

$$\mathcal{F}_v := \mathcal{P}\tilde{v}, \quad \mathcal{J}_v := \mathcal{B}\tilde{v}.$$

Thus, given the pair $\{\mathcal{F}_v, \mathcal{J}_v\}$ we had an *exact* solution of the nonhomogeneous problem, namely $\tilde{v}$. While this does not prove an implementation to be correct, if the function $\tilde{v}$ is chosen to imitate the behavior of anticipated solutions (e.g., satisfying the boundary conditions exactly), then this gives us confidence in our algorithm.

In the present setting we considered the prototype Maxwell problem (cf. (6.2)),

$$\mathcal{L}_0 \tilde{v} = F_v \qquad\qquad \text{in } S_v,$$
$$-\partial_z \tilde{v} - T_u[\tilde{v}] = Q_v \qquad\qquad \text{at } \Gamma_h,$$
$$\partial_z \tilde{v} - T_w[\tilde{v}] = R_v \qquad\qquad \text{at } \Gamma_{-h},$$
$$\tilde{v}(x + d_x, y + d_y, z) = e^{i\alpha d_x + i\beta d_y}\tilde{v}(x, y, z),$$

with

$$d_x = d_y = 2\pi, \quad h = 5/2, \quad k_0 = 1.3, \quad \theta = \phi = 0,$$

and the (biperiodic) manufactured solution,

$$\tilde{v}(x,y,z) = \begin{pmatrix} A_1 \\ A_2 \\ A_3 \end{pmatrix} e^{i\alpha_s x + i\beta_t y + i\bar{\gamma}_{s,t} z},$$

$$A_1 = 1, \quad A_2 = \frac{\pi}{4}, \quad A_3 = -\frac{A_1(i\alpha_s) + A_2(i\beta_t)}{i\bar{\gamma}_{s,t}}, \quad s = t = 1.$$

We coupled this with (essentially) the choice of envelope function mentioned above in section 4,

$$\bar{\epsilon} = 0.9, \quad \mathcal{E}(x,y,z) = \left(\frac{\bar{\epsilon} - \epsilon'}{\bar{\epsilon}}\right) \Phi_{-d,d}(z) \left\{1 - \Phi_{a,b}(x)\right\},$$

where we selected

$$a = \pi/2, \quad b = 3\pi/2, \quad d = 1/4, \quad \delta = 1.$$

For our test we supplied the "exact" input data, $\{F_v, Q_v, R_v\}$ to our HOPE algorithm and compared the output of this, $\tilde{v}^{\mathrm{approx}}$, with $\tilde{v}$ by computing the error

(8.2) $$\mathrm{Error} := |\tilde{v} - \tilde{v}^{\mathrm{approx}}|_{L^\infty}.$$

To evaluate our implementation and demonstrate the behavior of our scheme, we followed the lead of [27] and report on results in the "small deviation" ($\epsilon' = 1.1$) and "large deviation" ($\epsilon' = 1.6$) regimes. We further evaluated our scheme by studying the effect of the sharpness of the transition from $\bar{\epsilon}$ to ϵ' in $\mathcal{E}(x,y,z;w)$ by choosing $w = 2$ (smooth transition) and $w = 200$ (sharp transition).

8.3. Small deviation. In Figure 8.1 we display our results of simulations of the small deviation ($\epsilon' = 1.1$) configuration with transition parameter choices $w = 2$ (left) and $w = 200$ (right). In both figures we have selected $\delta = 1$ and $N_x = N_y = N_z = 24$, and we note the steady and stable convergence of our method. In both the smooth and sharp transition cases we realize an error of nearly machine zero (10^{-14}) by $L = 12$. This, of course, is in complete alignment with the results we have established above (section 6) on analyticity of the field with respect to the deviation parameter δ.

8.4. Large deviation. We repeated these simulations in the large deviation setting ($\epsilon' = 1.6$) and, in Figure 8.2, we exhibit our findings, again, with transition
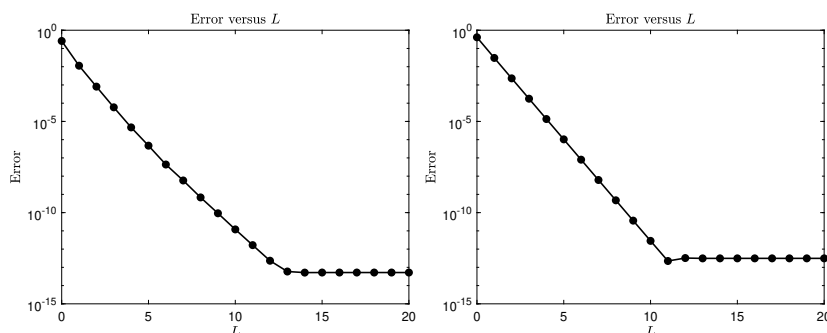

Fig. 8.1. *Error, (8.2), in HOPE simulation of small deviation configuration ($\epsilon' = 1.1$) with transition parameter $w = 2$ (left: smooth transition) and $w = 200$ (right: sharp transition) versus perturbation order L. ($N_x = N_y = N_z = 24$, $\delta = 1$.)*
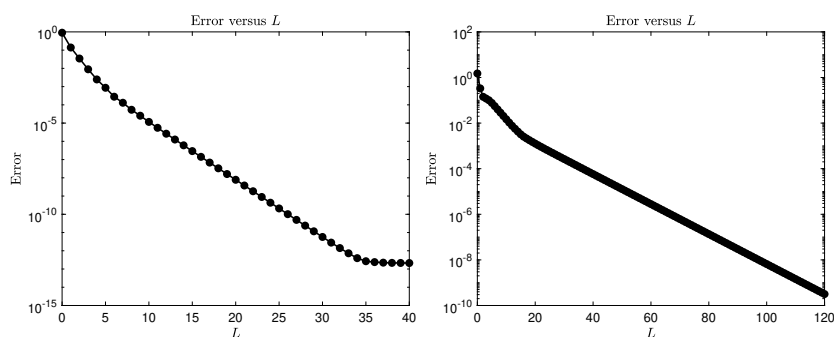
FIG. 8.2. *Error, (8.2), in HOPE simulation of large deviation configuration ($\epsilon' = 1.6$) with transition parameter $w = 2$ (left: smooth transition) and $w = 200$ (right: sharp transition) versus perturbation order L. ($N_x = N_y = N_z = 24$ ($w = 2$) and $N_x = N_y = N_z = 32$ ($w = 200$), $\delta = 1$.)*
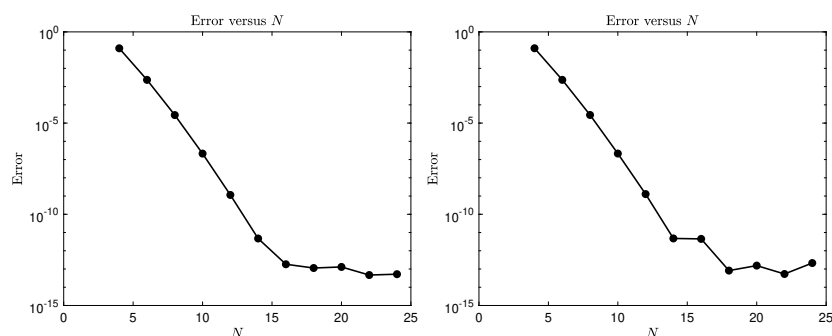

FIG. 8.3. *Error, (8.2), in HOPE simulation with transition parameter $w = 2$ for small deviation (left: $\epsilon' = 1.1$) and large deviation (right: $\epsilon' = 1.6$) versus $N_x = N_y = N_z$ ($L = 20$ ($\epsilon' = 1.1$), $L = 40$ ($\epsilon' = 1.6$), $\delta = 1$).*

parameter choices $w = 2$ (left) and $w = 200$ (right). As before, we selected $\delta = 1$ and $N_x = N_y = N_z = 24$ for $w = 2$. For $w = 200$ we chose $N_x = N_y = N_z = 32$ and note the steady and stable convergence of our method. Of course the results are less impressive in this much more challenging setting, but by $L = 40$ one can realize errors on the order of 10^{-14} for the smooth transition. In the case of the sharp transition we achieved errors of magnitude 10^{-10} with $L = 120$. As before this agrees completely with our novel analyticity results in section 6.

8.5. Spatial discretization. To close out our MMS simulations we *fixed* the perturbation order, L, and varied the spatial discretization parameters $N_x = N_y = N_z$ among values from 4 to 24. In Figure 8.3, we summarize our results in the case of a small deviation (left: $\epsilon' = 1.1$, $L = 20$) and large deviation (right: $\epsilon' = 1.6$, $L = 40$) with $w = 2$ at $\delta = 1$. In line with our joint analyticity results in section 7 we note the spectral rate of convergence of our simulations to errors of 10^{-14} and 10^{-13} for the smooth and sharp transitions, respectively, as $N_x = N_y = N_z$ increased from 4 to 24.

8.6. Energy defect. While our simulations with the MMS provide convincing evidence for the correctness, stability, and accuracy of our numerical implementation, they do not directly address the problem of plane-wave scattering we described in section 2. Of course this is by necessity as there is no closed-form solution for plane-wave scattering by a generic periodic structure. However, it is well-known that if the

structure is composed entirely of lossless media (so that $\mathrm{Im}\{\epsilon\} = 0$) there is a principle of conservation of energy [39] which is often used as a diagnostic of convergence (see, e.g., [30, 31]). The survey of Bao and Li [3, Chapter 2] gives an excellent derivation and rigorous proof of this result which we summarize here. Recalling from (2.2) the incident radiation

$$E^{\mathrm{inc}}(x,y,z) = A\exp(i\alpha x + i\beta y - i\gamma^{(u)}z),$$

and the Rayleigh expansions in the upper layer,

$$E^{\mathrm{refl}}(x,y,z) = \sum_{p=-\infty}^{\infty}\sum_{q=-\infty}^{\infty} \hat{u}_{p,q}\exp(i\alpha_p x + i\beta_q y + i\gamma_{p,q}^{(u)}z)$$

(cf. (3.1)), and lower layer,

$$E^{\mathrm{trans}}(x,y,z) = \sum_{p=-\infty}^{\infty}\sum_{q=-\infty}^{\infty} \hat{w}_{p,q}\exp(i\alpha_p x + i\beta_q y - i\gamma_{p,q}^{(w)}z)$$

(cf. (3.3)), we have the formulas for the (p,q)th reflected and transmitted efficiencies

$$r_{p,q} = \left(\frac{\gamma_{p,q}^{(u)}}{\gamma^{(u)}}\right)\frac{|\hat{u}_{p,q}|^2}{|A|^2}, \qquad (p,q)\in\mathcal{U}^{(u)},$$

$$t_{p,q} = \left(\frac{\gamma_{p,q}^{(w)}}{\gamma^{(u)}}\right)\frac{|\hat{w}_{p,q}|^2}{|A|^2}, \qquad (p,q)\in\mathcal{U}^{(w)},$$

where the sets of propagating modes are defined by

$$\mathcal{U}^{(m)} := \left\{(p,q)\in\mathbf{Z}^2 \mid \alpha_p^2 + \beta_q^2 \le \epsilon^{(m)}k_0^2\right\}, \quad m\in\{u,w\}.$$

Conservation of energy demands that

$$\sum_{(p,q)\in\mathcal{U}^{(u)}} r_{p,q} + \sum_{(p,q)\in\mathcal{U}^{(w)}} t_{p,q} = 1,$$

so that, in an ideal computation, the *energy defect*

$$(8.3) \qquad \Delta := 1 - \sum_{(p,q)\in\mathcal{U}^{(u)}} r_{p,q} - \sum_{(p,q)\in\mathcal{U}^{(w)}} t_{p,q}$$

should be identically zero. Of course, our numerical simulation will experience errors, but we can evaluate its capabilities for plane-wave scattering by studying Δ as the numerical parameters, $\{N_x, N_y, N_z, L\}$, are refined.

To compute these efficiencies we recall that we simulate $E = E(x,y,z)$, the total field, in S_v. Evaluating at Γ_h we find that

$$E(x,y,h) = E^{\mathrm{inc}}(x,y,h) + E^{\mathrm{refl}}(x,y,h)$$

$$= A\exp(i\alpha x + i\beta y - i\gamma^{(u)}h) + \sum_{p=-\infty}^{\infty}\sum_{q=-\infty}^{\infty} \hat{u}_{p,q}\exp(i\alpha_p x + i\beta_q y + i\gamma_{p,q}^{(u)}h),$$

so that

$$\hat{u}_{p,q} = \begin{cases} \exp(-i\gamma^{(u)}h)\left\{\widehat{E(\cdot,\cdot,h)}_{0,0} - A\exp(-i\gamma^{(u)}h)\right\}, & (p,q)=(0,0), \\ \exp(-i\gamma_{p,q}^{(u)}h)\widehat{E(\cdot,\cdot,h)}_{p,q}, & (p,q)\ne(0,0), \end{cases}$$

where $\widehat{E(\cdot,\cdot,h)}_{p,q}$ is the (p,q)th Fourier coefficient of $E(x,y,h)$. In a similar manner, evaluating E at Γ_{-h} we have

$$
\begin{aligned}
E(x,y,-h) &= E^{\text{trans}}(x,y,-h) \\
&= \sum_{p=-\infty}^{\infty} \sum_{q=-\infty}^{\infty} \hat{w}_{p,q} \exp(i\alpha_p x + i\beta_q y - i\gamma_{p,q}^{(w)}(-h)),
\end{aligned}
$$

so that

$$
\hat{w}_{p,q} = \exp(-i\gamma_{p,q}^{(w)} h) \left\{ \widehat{E(\cdot,\cdot,-h)}_{p,q} \right\},
$$

where $\widehat{E(\cdot,\cdot,-h)}_{p,q}$ is the (p,q)th Fourier coefficient of $E(x,y,-h)$.

With all of this in hand we can now revisit the computations we presented in sections 8.3, 8.4, and 8.5. Regarding the small deviation $\epsilon' = 1.1$ (cf. section 8.3), we present results for $w = 2$ and $w = 200$ in Figure 8.4. Here we see that after $L = 6$ orders we have achieved our best energy defect (10^{-9}) for $w = 2$, and by $L = 10$ orders we obtain the smallest discrepancy (10^{-15}) when $w = 200$.

For the large deviation $\epsilon' = 1.6$ (cf. section 8.4), our results for $w = 2$ and $w = 200$ are in Figure 8.5. Here we see that after $L = 9$ orders we have achieved our
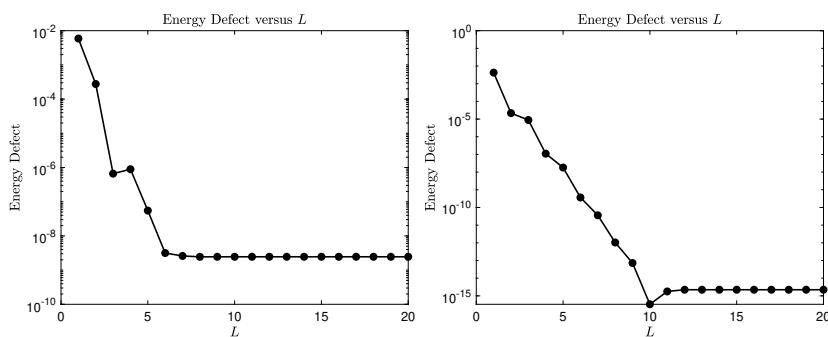

FIG. 8.4. *Energy defect, (8.3), in HOPE simulation of small deviation configuration ($\epsilon' = 1.1$) with transition parameter $w = 2$ (left: smooth transition) and $w = 200$ (right: sharp transition) versus perturbation order L. ($N_x = N_y = N_z = 24$, $\delta = 1$.)*
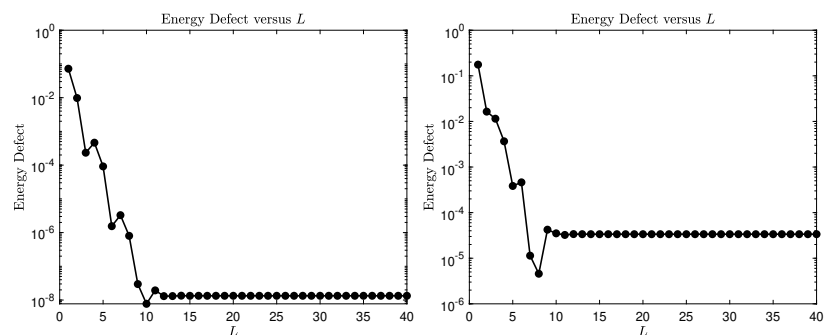

FIG. 8.5. *Energy defect, (8.3), in HOPE simulation of large deviation configuration ($\epsilon' = 1.6$) with transition parameter $w = 2$ (left: smooth transition) and $w = 200$ (right: sharp transition) versus perturbation order L. ($N_x = N_y = N_z = 24$, $\delta = 1$.)*
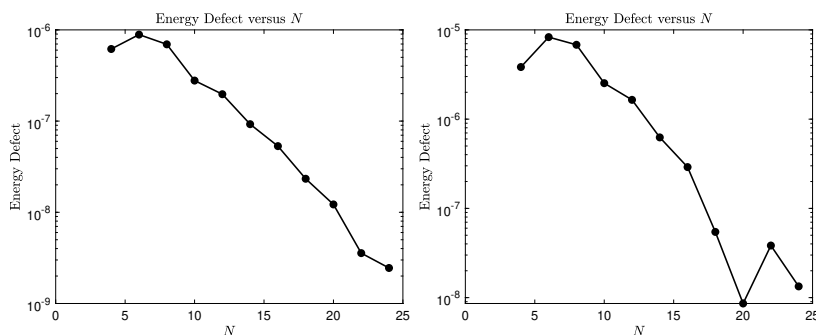
FIG. 8.6. *Energy defect, (8.3), in HOPE simulation with transition parameter $w = 2$ for small deviation (left: $\epsilon' = 1.1$) and large deviation (right: $\epsilon' = 1.6$) versus $N_x = N_y = N_z$ ($L = 20$ ($\epsilon' = 1.1$), $L = 40$ ($\epsilon' = 1.6$), $\delta = 1$).*

best energy defect (10^{-8}) for $w = 2$, and by $L = 11$ orders we obtain the smallest discrepancy (10^{-5}) when $w = 200$.

Finally, regarding the spatial discretization (cf. section 8.5), our results for $\epsilon' = 1.1$ and $\epsilon' = 1.6$ are displayed in Figure 8.6. Here we see that after $N = N_x = N_y = N_z = 24$ we have achieved our best energy defect (10^{-8}) for $\epsilon' = 1.1$, and by $N = N_x = N_y = N_z = 24$ we obtain the smallest discrepancy (10^{-5}) when $\epsilon' = 1.6$.

Appendix A. Proof of an elliptic estimate: Joint analyticity. In this appendix we establish the elliptic estimate, Theorem 7.3, required to prove joint analyticity of the scattered field using the inductive proof described in section 7. As our proof is inductive in the vertical, z, derivative, we begin with the following lateral regularity result.

THEOREM A.1. *Given any integer $m \geq 0$, if $(\omega, \bar{\epsilon}) \in \mathcal{P}$, $F(x, y, z) \in C_m^\omega(S_v)$ such that*

$$\max\left\{\left\|\frac{\partial_x^r \partial_y^t}{(r+t)!} F\right\|_{H^0}, \left\|\frac{\partial_x^r \partial_y^t}{(r+t)!} \mathrm{div}\,[F]\right\|_{H^1}\right\} \leq C_F \frac{\eta^r}{(r+1)^2} \frac{\theta^t}{(t+1)^2}$$

for all $r, t \geq 0$ and for some constants $C_F, \eta, \theta > 0$, and $Q, R \in C_m^\omega(\Gamma)$) satisfying

$$\left\|\frac{\partial_x^r \partial_y^t}{(r+t)!} Q\right\|_{H^{1/2}} \leq C_Q \frac{\eta^r}{(r+1)^2} \frac{\theta^t}{(t+1)^2},$$

$$\left\|\frac{\partial_x^r \partial_y^t}{(r+t)!} R\right\|_{H^{1/2}} \leq C_R \frac{\eta^r}{(r+1)^2} \frac{\theta^t}{(t+1)^2}$$

for all $r, t \geq 0$ and some constants $C_R, C_Q > 0$, then there exists a unique solution $v \in C_m^\omega(S_v)$ of

(A.1a)	$\mathcal{L}_0 v = F$	*in S_v,*
(A.1b)	$-\partial_z v - T_u[v] = Q$	*at Γ_h,*
(A.1c)	$\partial_z v - T_w[v] = R$	*at Γ_{-h},*
(A.1d)	$v(x + d_x, y + d_y, z) = e^{i\alpha d_x + i\beta d_y} v(x, y, z),$	

satisfying

$$\left\| \frac{\partial_x^r \partial_y^t}{(r+t)!} v \right\|_{H^2} \le \underline{C}_e \frac{\eta^r}{(r+1)^2} \frac{\theta^t}{(t+1)^2},$$

for all $r, t \ge 0$ where

$$\underline{C}_e = C_e (C_F + C_Q + C_R) > 0,$$

and $\overline{C}(h) > 0$ is a constant.

Proof. Applying the operator $\partial_x^r \partial_y^t / (r+t)!$ to (A.1) we obtain

$$
\begin{aligned}
\mathcal{L}_0 \left[\frac{\partial_x^r \partial_y^t}{(r+t)!} v \right] &= \frac{\partial_x^r \partial_y^t}{(r+t)!} F & \text{in } S_v, \\
-\partial_z \left[\frac{\partial_x^r \partial_y^t}{(r+t)!} v \right] - T_u \left[\frac{\partial_x^r \partial_y^t}{(r+t)!} v \right] &= \frac{\partial_x^r \partial_y^t}{(r+t)!} Q & \text{at } \Gamma_h, \\
\partial_z \left[\frac{\partial_x^r \partial_y^t}{(r+t)!} v \right] - T_w \left[\frac{\partial_x^r \partial_y^t}{(r+t)!} v \right] &= \frac{\partial_x^r \partial_y^t}{(r+t)!} R & \text{at } \Gamma_{-h}, \\
\frac{\partial_x^r \partial_y^t}{(r+t)!} v(x + d_x, y + d_y, z) &= e^{i\alpha d_x + i\beta d_y} \frac{\partial_x^r \partial_y^t}{(r+t)!} v(x, y, z).
\end{aligned}
$$

Applying Theorem 6.1 to this system and using the hypothesis on F, Q, and R, we obtain

$$
\begin{aligned}
\left\| \frac{\partial_x^r \partial_y^t}{(r+t)!} v \right\|_{H^2} \le\ & C_e \left(\left\| \frac{\partial_x^r \partial_y^t}{(r+t)!} F \right\|_{H^0} + \left\| \mathrm{div} \left[\frac{\partial_x^r \partial_y^t}{(r+t)!} F \right] \right\|_{H^1} \right. \\
& \left. + \left\| \frac{\partial_x^r \partial_y^t}{(r+t)!} Q \right\|_{H^{1/2}} + \left\| \frac{\partial_x^r \partial_y^t}{(r+t)!} R \right\|_{H^{1/2}} \right) \\
\le\ & C_e (C_F + C_Q + C_R) \frac{\eta^r}{(r+1)^2} \frac{\theta^t}{(t+1)^2},
\end{aligned}
$$

and we are done by choosing $\underline{C}_e = C_e(C_F + C_Q + C_R)$. $\qquad\square$

We are now in a position to establish our main result.

Proof of Theorem 7.3. We prove (7.1) by induction in s, and the case $s = 0$ is verified by the previous result, Theorem A.1. We now assume that

$$\left\| \frac{\partial_x^r \partial_y^t \partial_z^s}{(r+t+s)!} v \right\|_{H^2} \le \underline{C}_e \frac{\eta^r}{(r+1)^2} \frac{\theta^t}{(t+1)^2} \frac{\zeta^s}{(s+1)^2} \quad \forall\, s < \overline{s}, \quad \forall\, r, t \ge 0,$$

which implies that, for $j \in \{x, y, z\}$,

$$\left\| \frac{\partial_x^r \partial_y^t \partial_z^s}{(r+t+s)!} v^j \right\|_{H^2} \le \underline{C}_e \frac{\eta^r}{(r+1)^2} \frac{\theta^t}{(t+1)^2} \frac{\zeta^s}{(s+1)^2} \quad \forall\, s < \overline{s}, \quad \forall\, r, t \ge 0.$$

We now examine

$$\left\|\frac{\partial_x^r\partial_y^t\partial_z^{\overline{s}}}{(r+t+\overline{s})!}v\right\|_{H^2} \leq \left\|\frac{\partial_x^r\partial_y^t\partial_z^{\overline{s}}}{(r+t+\overline{s})!}v\right\|_{H^1} + \left\|\frac{\partial_x^r\partial_y^t\partial_z^{\overline{s}}}{(r+t+\overline{s})!}\partial_x v\right\|_{H^1}$$

$$+ \left\|\frac{\partial_x^r\partial_y^t\partial_z^{\overline{s}}}{(r+t+\overline{s})!}\partial_y v\right\|_{H^1} + \left\|\frac{\partial_x^r\partial_y^t\partial_z^{\overline{s}}}{(r+t+\overline{s})!}\partial_z v\right\|_{H^1}$$

$$\leq \left\|\frac{\partial_x^r\partial_y^t\partial_z^{\overline{s}-1}}{(r+t+\overline{s})!}v\right\|_{H^2} + \left\|\frac{\partial_x^r\partial_y^t\partial_z^{\overline{s}-1}}{(r+t+\overline{s})!}\partial_x v\right\|_{H^2}$$

$$+ \left\|\frac{\partial_x^r\partial_y^t\partial_z^{\overline{s}-1}}{(r+t+\overline{s})!}\partial_y v\right\|_{H^2} + \left\|\frac{\partial_x^r\partial_y^t\partial_z^{\overline{s}-1}}{(r+t+\overline{s})!}\partial_z^2 v\right\|_{H^1}.$$

The first three terms can be bounded by our inductive hypothesis as they involve z derivatives of order $\overline{s}-1$. The fourth term we denote W and analyze as follows. Writing

$$W^j := \left\|\frac{\partial_x^r\partial_y^t\partial_z^{\overline{s}-1}}{(r+t+\overline{s})!}\partial_z^2 v^j\right\|_{H^1}, \quad j \in \{x,y,z\},$$

it is clear that $W \leq W^x + W^y + W^z$. To estimate W^x and W^y we recall that the inhomogeneous Maxwell equations

$$-\Delta v + \nabla\mathrm{div}\;[v] - k_0^2\overline{\epsilon}v = F$$

give

$$\partial_z^2 v = -F - k_0^2\overline{\epsilon}v - \partial_x^2 v - \partial_y^2 v + \begin{pmatrix}\partial_x(\partial_x v^x + \partial_y v^y + \partial_z v^z)\\\partial_y(\partial_x v^x + \partial_y v^y + \partial_z v^z)\\\partial_z(\partial_x v^x + \partial_y v^y + \partial_z v^z)\end{pmatrix}.$$

Therefore, we can write $\partial_z^2 v^x$ and $\partial_z^2 v^y$ as

$$\partial_z^2 v^x = -F^x - k_0^2\overline{\epsilon}v^x - \partial_y^2 v^x + \partial_x\partial_y v^y + \partial_x\partial_z v^z,$$
$$\partial_z^2 v^y = -F^y - k_0^2\overline{\epsilon}v^y - \partial_x^2 v^y + \partial_x\partial_y v^x + \partial_y\partial_z v^z.$$

With these and the inductive hypothesis on v we obtain

$$W^x \leq \left\|\frac{\partial_x^r\partial_y^t\partial_z^{\overline{s}-1}}{(r+t+\overline{s})!}F^x\right\|_{H^1} + k_0^2\overline{\epsilon}\left\|\frac{\partial_x^r\partial_y^t\partial_z^{\overline{s}-1}}{(r+t+\overline{s})!}v^x\right\|_{H^1} + \left\|\frac{\partial_x^r\partial_y^{t+1}\partial_z^{\overline{s}-1}}{(r+t+\overline{s})!}\partial_y v^x\right\|_{H^1}$$

$$+ \left\|\frac{\partial_x^r\partial_y^{t+1}\partial_z^{\overline{s}-1}}{(r+t+\overline{s})!}\partial_x v^y\right\|_{H^1} + \left\|\frac{\partial_x^{r+1}\partial_y^t\partial_z^{\overline{s}-1}}{(r+t+\overline{s})!}\partial_z v^z\right\|_{H^1}$$

$$\leq \left\|\frac{\partial_x^r\partial_y^t\partial_z^{\overline{s}-1}}{(r+t+\overline{s})!}F^x\right\|_{H^2} + k_0^2\overline{\epsilon}\left\|\frac{\partial_x^r\partial_y^t\partial_z^{\overline{s}-1}}{(r+t+\overline{s})!}v^x\right\|_{H^2} + \left\|\frac{\partial_x^r\partial_y^{t+1}\partial_z^{\overline{s}-1}}{(r+t+\overline{s})!}v^x\right\|_{H^2}$$

$$+ \left\|\frac{\partial_x^r\partial_y^{t+1}\partial_z^{\overline{s}-1}}{(r+t+\overline{s})!}v^y\right\|_{H^2} + \left\|\frac{\partial_x^{r+1}\partial_y^t\partial_z^{\overline{s}-1}}{(r+t+\overline{s})!}v^z\right\|_{H^2}$$

$$\leq \underline{C_e}\frac{\eta^r}{(r+1)^2}\frac{\theta^t}{(t+1)^2}\frac{\zeta^{\overline{s}}}{(\overline{s}+1)^2}\left(\frac{2\theta}{\zeta}\frac{(t+1)^2}{(t+2)^2}\frac{(\overline{s}+1)^2}{\overline{s}^2} + \frac{\eta}{\zeta}\frac{(r+1)^2}{(r+2)^2}\frac{(\overline{s}+1)^2}{\overline{s}^2}\right)$$

$$\leq \underline{C_e}\frac{\eta^r}{(r+1)^2}\frac{\theta^t}{(t+1)^2}\frac{\zeta^{\overline{s}}}{(\overline{s}+1)^2}\left(\frac{8\theta+4\eta}{\zeta}\right),$$

where the last inequality is obtained by using the inequalities

$$\frac{(\overline{s}+1)^2}{\overline{s}^2} \le 4, \quad \frac{(t+1)^2}{(t+2)^2} \le 1.$$

In analogous fashion we obtain

$$W^y \le \underline{C_e} \frac{\eta^r}{(r+1)^2} \frac{\theta^t}{(t+1)^2} \frac{\zeta^{\overline{s}}}{(\overline{s}+1)^2} \left(\frac{8\theta+4\eta}{\zeta}\right).$$

All that remains is to estimate W^z, which we accomplish by applying the divergence operator to the Maxwell equations (noting that div $[\text{curl}[\psi]] = 0$ for any ψ), giving

$$-k_0^2 \overline{\epsilon} \text{div } [v] = \text{div } F,$$

which implies that

$$\partial_z v^z = -\frac{1}{k_0^2 \overline{\epsilon}} \text{div } [F] - \partial_x v^x - \partial_y v^y$$

and

$$\partial_z^2 v^z = -\frac{1}{k_0^2 \overline{\epsilon}} \partial_z \text{div } [F] - \partial_x \partial_z v^x - \partial_y \partial_z v^y.$$

Therefore,

$$W^z \le \frac{1}{k_0^2 \overline{\epsilon}} \left\| \frac{\partial_x^r \partial_y^t \partial_z^{\overline{s}-1}}{(r+t+\overline{s})!} \partial_z \text{div } [F] \right\|_{H^1} + \left\| \frac{\partial_x^{r+1} \partial_y^t \partial_z^{\overline{s}-1}}{(r+t+\overline{s})!} \partial_z v^x \right\|_{H^1} + \left\| \frac{\partial_x^r \partial_y^{t+1} \partial_z^{\overline{s}-1}}{(r+t+\overline{s})!} \partial_z v^y \right\|_{H^1}$$

$$\le \frac{1}{k_0^2 \overline{\epsilon}} \left\| \frac{\partial_x^r \partial_y^t \partial_z^{\overline{s}-1}}{(r+t+\overline{s})!} \partial_z \text{div } [F] \right\|_{H^1} + \left\| \frac{\partial_x^{r+1} \partial_y^t \partial_z^{\overline{s}-1}}{(r+t+\overline{s})!} v^x \right\|_{H^2} + \left\| \frac{\partial_x^r \partial_y^{t+1} \partial_z^{\overline{s}-1}}{(r+t+\overline{s})!} v^y \right\|_{H^2}.$$

The first term is readily estimated from the hypothesis of F. The second and third terms can be addressed by our inductive hypothesis for v^x and v^y as they just involve z derivatives of order $\overline{s} - 1$. Thus, we obtain

$$W^z \le \underline{C_e} \frac{\eta^r}{(r+1)^2} \frac{\theta^t}{(t+1)^2} \frac{\zeta^{\overline{s}}}{(\overline{s}+1)^2} \left(\frac{4\theta+4\eta}{\zeta}\right).$$

Finally, collecting all the estimates for W^x, W^y, and W^z, we arrive at

$$W^x + W^y + W^z \le \underline{C_e} \frac{\eta^r}{(r+1)^2} \frac{\theta^t}{(t+1)^2} \frac{\zeta^{\overline{s}}}{(\overline{s}+1)^2} \left(\frac{20\theta+12\eta}{\zeta}\right).$$

The proof is complete by choosing $\zeta \ge 20\theta + 12\eta$. $\qquad \square$

REFERENCES

[1] T. ARENS, *Scattering by Biperiodic Layered Media: The Integral Equation Approach*, Habilitationsschrift, Karlsruhe Institute of Technology, 2009.

[2] G. A. BAKER, JR., AND P. GRAVES-MORRIS, *Padé Approximants*, 2nd ed., Cambridge University Press, Cambridge, UK, 1996.

[3] G. BAO AND P. LI, *Maxwell's Equations in Periodic Structures*, Appl. Math. Sci. 208, Springer, Beijing, 2022.

[4] J. P. BOYD, *Chebyshev and Fourier Spectral Methods*, 2nd ed., Dovers, Mineola, NY, 2001.

[5] O. R. BURGGRAF, *Analytical and numerical studies of the structure of steady separated flows*, J. Fluid Mech., 24 (1966), pp. 113–151, https://doi.org/10.1017/S0022112066000545.

[6] C. CANUTO, M. Y. HUSSAINI, A. QUARTERONI, AND T. A. ZANG, *Spectral Methods in Fluid Dynamics*, Springer-Verlag, New York, 1988.

[7] D. COLTON AND R. KRESS, *Inverse Acoustic and Electromagnetic Scattering Theory*, 3rd ed., Appl. Math. Sci. 93, Springer, New York, 2013.

[8] M. O. DEVILLE, P. F. FISCHER, AND E. H. MUND, *High-Order Methods for Incompressible Fluid Flow*, Cambridge Monogr. Appl. Comput. Math. 9, Cambridge University Press, Cambridge, UK, 2002.

[9] T. W. EBBESEN, H. J. LEZEC, H. F. GHAEMI, T. THIO, AND P. A. WOLFF, *Extraordinary optical transmission through sub-wavelength hole arrays*, Nature, 391 (1998), pp. 667–669, https://doi.org/10.1038/35570.

[10] I. EL-SAYED, X. HUANG, AND M. EL-SAYED, *Selective laser photo-thermal therapy of epithelial carcinoma using anti-EGFR antibody conjugated gold nanoparticles*, Cancer Lett., 239 (2006), pp. 129–135, https://doi.org/10.1016/j.canlet.2005.07.035.

[11] O. G. ERNST AND M. J. GANDER, *Why it is difficult to solve Helmholtz problems with classical iterative methods*, in Numerical Analysis of Multiscale Problems, Lect. Notes Comput. Sci. Eng. 83, Springer, Heidelberg, 2012, pp. 325–363.

[12] L. C. EVANS, *Partial Differential Equations*, 2nd ed., AMS, Providence, RI, 2010.

[13] X. FENG, J. LIN, AND C. LORTON, *An efficient numerical method for acoustic wave scattering in random media*, SIAM/ASA J. Uncertain. Quantif., 3 (2015), pp. 790–822, https://doi.org/10.1137/140958232.

[14] X. FENG, J. LIN, AND C. LORTON, *A multimodes Monte Carlo finite element method for elliptic partial differential equations with random coefficients*, Int. J. Uncertain. Quantif., 6 (2016), pp. 429–443, https://doi.org/10.1615/Int.J.UncertaintyQuantification.2016016805.

[15] D. GOTTLIEB AND S. A. ORSZAG, *Numerical Analysis of Spectral Methods: Theory and Applications*, CBMS-NSF Regional Conf. Ser. in Appl. Math. 26, SIAM, Philadelphia, 1977, https://doi.org/10.1137/1.9781611970425.

[16] J. S. HESTHAVEN AND T. WARBURTON, *Nodal Discontinuous Galerkin Methods: Algorithms, Analysis, and Applications*, Texts in Appl. Math. 54, Springer, New York, 2008.

[17] J. HOMOLA, *Surface plasmon resonance sensors for detection of chemical and biological species*, Chem. Rev., 108 (2008), pp. 462–493, https://doi.org/10.1021/cr068107d.

[18] Y. HONG AND D. NICHOLLS, *A rigorous numerical analysis of the transformed field expansion method for diffraction by periodic, layered structures*, SIAM J. Numer. Anal., 59 (2021), pp. 456–476, https://doi.org/10.1137/20M131374X.

[19] F. IHLENBURG, *Finite Element Analysis of Acoustic Scattering*, Springer-Verlag, New York, 1998.

[20] C. JOHNSON, *Numerical Solution of Partial Differential Equations by the Finite Element Method*, Cambridge University Press, Cambridge, UK, 1987.

[21] J. JOSE, L. R. JORDAN, T. W. JOHNSON, S. H. LEE, N. J. WITTENBERG, AND S.-H. OH, *Topographically flat substrates with embedded nanoplasmonic devices for biosensing*, Adv. Funct. Mater, 23 (2013), pp. 2812–2820, https://doi.org/10.1002/adfm.201202214.

[22] R. KRESS, *Linear Integral Equations*, 3rd ed., Springer-Verlag, New York, 2014.

[23] R. J. LEVEQUE, *Finite Difference Methods for Ordinary and Partial Differential Equations: Steady-State and Time-Dependent Problems*, SIAM, Philadelphia, 2007.

[24] N. C. LINDQUIST, T. W. JOHNSON, J. JOSE, L. M. OTTO, AND S.-H. OH, *Ultrasmooth metallic films with buried nanostructures for backside reflection-mode plasmonic biosensing*, Ann. Phys., 524 (2012), pp. 687–696, https://doi.org/10.1002/andp.201200144.

[25] A. MOIOLA AND E. A. SPENCE, *Is the Helmholtz equation really sign-indefinite?*, SIAM Rev., 56 (2014), pp. 274–312, https://doi.org/10.1137/120901301.

[26] M. MOSKOVITS, *Surface–enhanced spectroscopy*, Rev. Modern Phys., 57 (1985), pp. 783–826, https://doi.org/10.1103/RevModPhys.57.783.

[27] D. P. NICHOLLS, *A high-order perturbation of envelopes (HOPE) method for scattering by periodic inhomogeneous media*, Quart. Appl. Math., 78 (2020), pp. 725–757, https://doi.org/10.1090/qam/1568.

[28] D. P. NICHOLLS AND F. REITICH, *A new approach to analyticity of Dirichlet-Neumann operators*, Proc. Roy. Soc. Edinburgh Sect. A, 131 (2001), pp. 1411–1433, https://doi.org/10.1017/S0308210500001463.

[29] D. P. NICHOLLS AND F. REITICH, *Analytic continuation of Dirichlet-Neumann operators*, Numer. Math., 94 (2003), pp. 107–146, https://doi.org/10.1007/s002110200399.

[30] D. P. Nicholls and F. Reitich, *Shape deformations in rough surface scattering: Cancellations, conditioning, and convergence*, J. Opt. Soc. Am. A, 21 (2004), pp. 590–605, https://doi.org/10.1364/JOSAA.21.000590.

[31] D. P. Nicholls and F. Reitich, *Shape deformations in rough surface scattering: Improved algorithms*, J. Opt. Soc. Am. A, 21 (2004), pp. 606–621, https://doi.org/10.1364/JOSAA.21.000606.

[32] D. P. Nicholls, F. Reitich, T. W. Johnson, and S.-H. Oh, *Fast high-order perturbation of surfaces (HOPS) methods for simulation of multilayer plasmonic devices and metamaterials*, J. Opt. Soc. Amer. A, 31 (2014), pp. 1820–1831, https://doi.org/10.1364/JOSAA.31.001820.

[33] R. Petit, ed., *Electromagnetic Theory of Gratings*, Springer-Verlag, Berlin, 1980.

[34] P. J. Roache, *Code verification by the method of manufactured solutions*, J. Fluids Eng., 124 (2002), pp. 4–10, https://doi.org/10.1115/1.1436090.

[35] C. J. Roy, *Review of code and solution verification procedures for computational simulation*, J. Comput. Phys., 205 (2005), pp. 131–156, https://doi.org/10.1016/j.jcp.2004.10.036.

[36] S. A. Sauter and C. Schwab, *Boundary Element Methods*, Springer Ser. Comput. Math. 39, Springer-Verlag, Berlin, 2011.

[37] J. Shen, T. Tang, and L.-L. Wang, *Spectral Methods: Algorithms, Analysis and Applications*, Springer Ser. Comput. Math. 41, Springer, Heidelberg, 2011.

[38] J. C. Strikwerda, *Finite Difference Schemes and Partial Differential Equations*, 2nd ed., SIAM, Philadelphia, 2004.

[39] P. Yeh, *Optical Waves in Layered Media*, Wiley Ser. Pure Appl. Optics 61, Wiley-Interscience, 2005.